JOURNAL OF MATERIALS SCIENCE 30 (1995) 4263–4272

Electromechanical and electrothermal behaviours of carbon whisker reinforced elastomer composites

VENKATESH CHELLAPPA, ZEN W. CHIOU, BOR Z. JANG*
Center for Materials Research and Education, 204 Wilmore Laboratory, Auburn University, Auburn, AL 36849, USA

The electromechanical and electrothermal properties of conducting carbon whisker reinforced thermoplastic elastomer (TPE) composites were investigated. The carbon whiskers were derived by a catalytic chemical vapour Deposition (CCVD) process and the TPE was a styrene–ethylene–butylene–styrene (S–EB–S) block copolymer. The electrical resistivity (ρ) of the composites can be varied either by uniaxial deformation (10^1–$10^8\,\Omega$ cm) or by temperature (10^1–$10^5\,\Omega$ cm). The temperature–resistivity studies indicated that the resistivity of these composites was influenced by the glass transition temperature (T_g) of the TPE. The ρ versus $1/T$ curves exhibited two distinct regimes each with a different negative slope which intersected at the T_g of the elastomer. This was correlated to the T_g of the EB segments in the S–EB–S block copolymer (~ -50°C) by the dynamic mechanical thermal analysis. Further, uniaxial deformation studies at room temperature (20 °C) demonstrated that the resistivity increased exponentially with the deformation. Processing technique considerations and electron micrographs of the morphology of the composites indicated the formation of polymeric film on the carbon whiskers. Thus, the electrical conduction between carbon whiskers in these highly loaded (33 and 52 vol% fraction) composites occurred through the elastomeric film by electron tunnelling. This is explained on the basis of Mott's electron hopping theory, for conduction through several carbon–polymer–carbon (C–P–C) junctions. Further studies by scanning electron microscopy, dielectric thermal analysis and voltage–current characteristics confirmed this observation. Mechanical and electrical properties of the composites indicated that CCVD carbon whiskers can be used to improve the strength and electrical conductivity of TPEs. The change in resistivity (up to five orders of magnitude) of the composites with respect to the deformation or temperature can find use in electromechanical and electrothermal device applications.

1. Introduction

Conducting carbon filler reinforced polymeric composites have attracted much attention because of their vast potential applications in electrostatic charge dissipators, electromagnetic shielding, electrodes for carbon–polymer batteries, flexible variacs, pressure sensors, potentiometers, etc. [1–5] These carbon fillers are essentially good conductors and the electrical behaviour of these composites can be modelled with a combination of conductor–insulator elements [6]. At above a certain critical volume concentration (> 30 vol % fraction) of the carbon filler, also known as the percolation threshold, the sample changes from an insulator ($\rho \gg 10^6\,\Omega$ cm) to a conductor ($10^1 \sim 10^0\,\Omega$ cm). The percolation threshold depends on the type of carbon, polymer, and the bonding between the two. Much work has been done on the percolation threshold theory [7–9] also known as the filamentary conduction mechanism. The sudden transition from an insulator to a conductor is similar to a second order phase transition and has been treated as such by Kirkpatrick [10].

The percolation theory can predict the change in resistivity reasonably well from the filler aspect ratio and volume concentration. However, for a highly loaded system (i.e. above a percolation threshold) the electrical properties cannot be fully explained on the basis of percolation threshold theory. Hence in the present study, an attempt has been made to explain the direct current (d.c.) conduction behaviour of highly loaded composite systems on the basis of the electron tunnelling phenomenon. The electron tunnelling phenomenon is based on the microstructural observation of the composites, i.e. the formation of possible carbon–polymer–carbon junctions (C–P–C).

A new class of carbon whiskers which were grown by the catalytic chemical vapour deposition (CCVD) technique was chosen as the reinforcing filler. Carbon whiskers can be grown by the decomposition of a hydrocarbon gas in the presence of a catalyst at as low as

* Author to whom all correspondence should be addressed.

0022–2461

300 °C and up to 2500 °C [11–13]. The morphology and the electrical resistivity of the resulting whiskers depend on several factors such as the nature of the hydrocarbon gas, catalyst and the deposition temperature. The electrical behaviour of these quasi-graphitic whiskers in the temperature range of 400 to 600 °C is not clearly understood. The resistivity of powdered and pelletized carbon whiskers grown at high temperatures (> 1000 °C) by a similar process was found to be in the range of 3–6 Ω cm [14]. The electrical behaviour of carbon fibres derived from organic fibres in the temperature range of 400 to 600 °C have exhibited semi-conducting properties [15–17]. The electrical behaviour of low temperature CCVD carbon whiskers (i.e. between 400 and 800 °C) is expected to be in the semiconducting range and they may behave quite differently than their graphitic counterparts. The addition of these whiskers as a reinforcing agent is influenced by the nature of the whiskers themselves and the adhesion between the matrix and the whiskers.

Thermoplastic elastomer (TPE) was chosen as the matrix material because of its large tensile strain property. Further, TPEs are gaining wide acceptance over their thermoset counterparts because of their processability and recyclability. The main purpose of this study was to obtain a better understanding of the electrical conduction mechanisms in the highly loaded CCVD carbon whisker–TPE composites and to identify their potential applications in electromechanical and electrothermal devices.

2. Experimental procedure

2.1. Processing of CCVD carbon whisker–elastomer composites

The carbon whiskers were grown by decomposing ethylene (C_2H_4) gas in the presence of Cu–Ni catalysts, a process developed at Auburn University [18]. CCVD carbon whiskers used in this study were grown at 400, 500 and 600 °C. The whisker–elastomer composites were made from two different whisker volume concentrations (33 and 52%). The TPE is a styrene–ethylene–butylene–styrene block copolymer under the trade name Kraton G1901X^{R}, with tensile strength of 0.1 MPa and resistivity $\approx 10^{12}$ Ω cm. The whiskers were mixed with the TPE pellets, dissolved in chloroform and then solution cast as thin sheets on a glass plate. The solvent was removed from the composites by placing the samples in a vacuum oven for 12 h at 1.333×10^2 Pa.

2.2. Morphology of CCVD carbon whisker–elastomer composites

Prior to processing, the representative samples of carbon whiskers were characterized by X-ray diffraction and scanning electron microscopy (SEM) to identify the degree of graphitization and their respective morphology. The composites were also characterized by SEM to observe the morphology developed under different CCVD carbon whiskers and their volume concentrations. The composite samples were slightly etched on the surface by chloroform and then gold sputtered before observing by SEM.

2.3. Characterization of CCVD carbon whisker–elastomer composites

2.3.1. Dynamic mechanical thermal analysis (DMTA)

Samples of dimensions ($7 \times 30 \times t$ mm) were cut from solution cast sheets for DMTA analysis. DMTA tests were performed on a dual cantilever configuration at 1 Hz frequency from −100 °C to 0 °C at a heating rate of 3 °C min^{-1}. The glass transition temperature T_g was determined by observing the change in complex Young's modulus E^* or tan δ with respect to temperature. The complex Young's modulus E^*, is given by $E^* = E' + iE'' = E'[1 + iE''/E'] = E'[1 + i \tan \delta]$, where $i = \sqrt{-1}$, and where E' = the storage modulus and E'' = the loss modulus. The T_g is defined as the temperature at which the loss tangent (tan δ) assumes a maximum value, where δ is the angle between the in-phase and out-of-phase components in the cyclic motion.

2.3.2. Dielectric thermal analysis (DETA)

DETA of the TPE and the composites were performed on a 33-mm diameter sample at 20 Hz frequency with an applied voltage of 1 V. The experiment was conducted from −100 to 50 °C at a heating rate of 2 °C min^{-1}. The dielectric constant (ε*), dielectric loss tangent (tan Δ) and the capacitance (C) were determined as follows: $\varepsilon^* = \varepsilon' - i\varepsilon''$, $\tan \Delta = \varepsilon''/\varepsilon'$ and $C = (\varepsilon_0 \varepsilon^*) A/d$, where ε'' = measure of loss current, ε' = measure of charging current, ε_0 = permittivity in vacuum ($8.85 \times 10^{-12} C^2/N m^{-2}$), A = cross-sectional area and d = the thickness of the sample.

2.4. Testing procedure

2.4.1. Tensile test

The samples (60 × 10 mm) for the tensile tests were cut from solution cast sheets. The thickness of the samples varied from batch to batch. The tensile test was performed at room temperature (≈20 °C) in an Instron testing machine under a constant cross-head rate of 5 cm min^{-1}, with the bulk resistance of the sample being measured simultaneously. The contact leads were attached to the Instron tensile grips as shown in Fig. 1, and the resistance was measured at regular intervals with a Keithely electrometer. The resistivity (ρ, Ω cm) was calculated for different strain values according to $\rho = R(A/L)$ where R = the bulk resistance, A = the cross-sectional area and L = the length of the sample. All the samples were tested till they failed. The fracture surface of the samples were prepared for failure analysis studies by SEM.

2.4.2. Temperature–resistivity studies

Samples of the same dimensions as above were used to study the change in resistivity as a function of temperature over a temperature range of −200 °C to 100 °C.

The samples were maintained at the desired temperature for 30 min to ensure a stable reading.

2.4.3. V–I characteristics

Internal field emissions [19] and the associated non-ohmic behaviour can shed some light on the conduction mechanism of filler reinforced composites. Hence, a continuous plot of voltage (up to 100 V) versus current was obtained for all the composites at 20 °C in a HP-1086 semi-conductor parameter analyser.

3. Results

3.1. CCVD carbon whisker characteristics

X-ray diffraction results of CCVD carbon whiskers are shown in Fig. 2. The intensity peaks at a 2Θ value of 26° and 45° correspond to the (0 0 2) and (1 0 0) graphitic peaks, respectively. The degree of graphitization in CCVD carbon whiskers increase with the deposition temperature. The intrinsic resistivity of pre-graphitic samples depends on the intensity of the (0 0 2) peak. Hence, the resistivity of 600 °C-grown whiskers is expected to be lower than those of the 500 °C and 400 °C grown whiskers. However, the bulk resistivity of the composite depends not only on the intrinsic conductivity of the whiskers, but also on the volume concentration and spatial distribution of the whiskers in the composites (Table I).

The morphology of the three CCVD carbon whiskers is shown in Fig. 3. The diameter of the carbon filament increases with the increase in deposition temperature. The 400°C CCVD whiskers appear like sponge (highly twisted and coiled) and the average diameter of the filament is ≈0.25 μm. The 500 °C CCVD whiskers also exhibit twisted filament morphology but the average filament diameter is slightly higher and more uniform in size. The 600°C CCVD whiskers exhibit intertwined filaments with an average

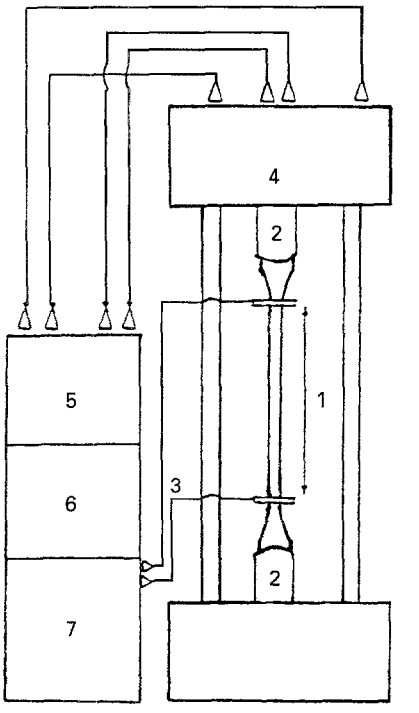

Figure 1 Experimental set-up for resistance measurement under uniaxial deformation. 1. Gauge length; 2. tensile grips; 3. voltage measurement set-up; 4. load cell; 5. controller; 6. load-displacement chart recorder; 7. digital electrometer.

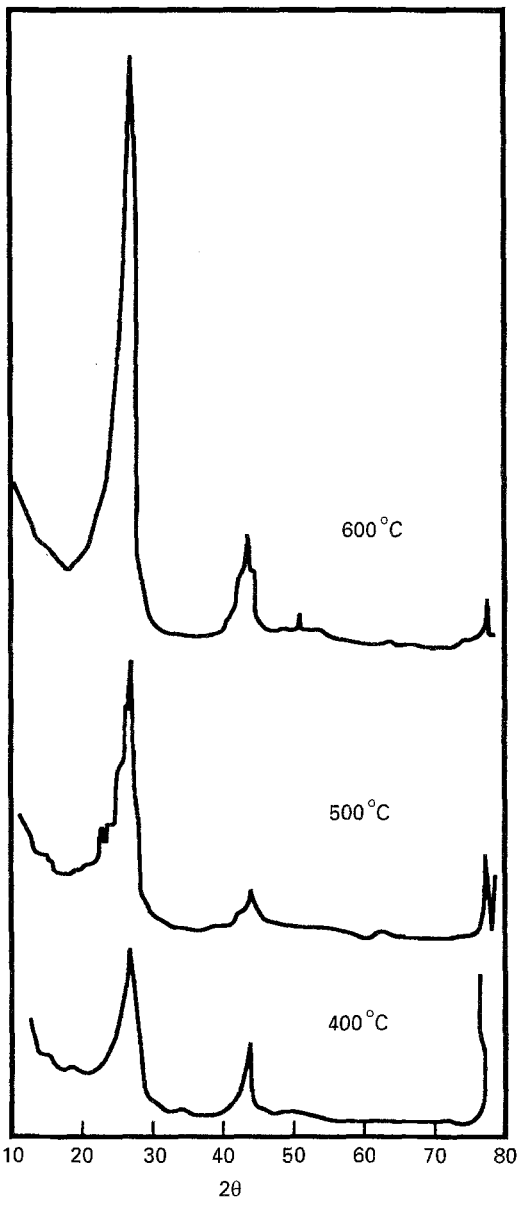

Figure 2 X-ray diffraction spectrum of CCVD carbon whiskers.

TABLE I Mechanical properties of carbon whisker–elastomer composites

Vol fraction (%)	Temperature (°C)	Tensile modulus (GPa)	Tensile strength (MPa)	Failure strain (%)
33	600	8.03 ± 1.01	1.66 ± 0.025	256 ± 68
33	500	3.87 ± 0.18	4.75 ± 0.05	1850 ± 100
52	500	13.22 ± 0.15	3.23 ± 0.12	60 ± 5
52	400	10.57 ± 0.28	4.53 ± 0.07	518 ± 37

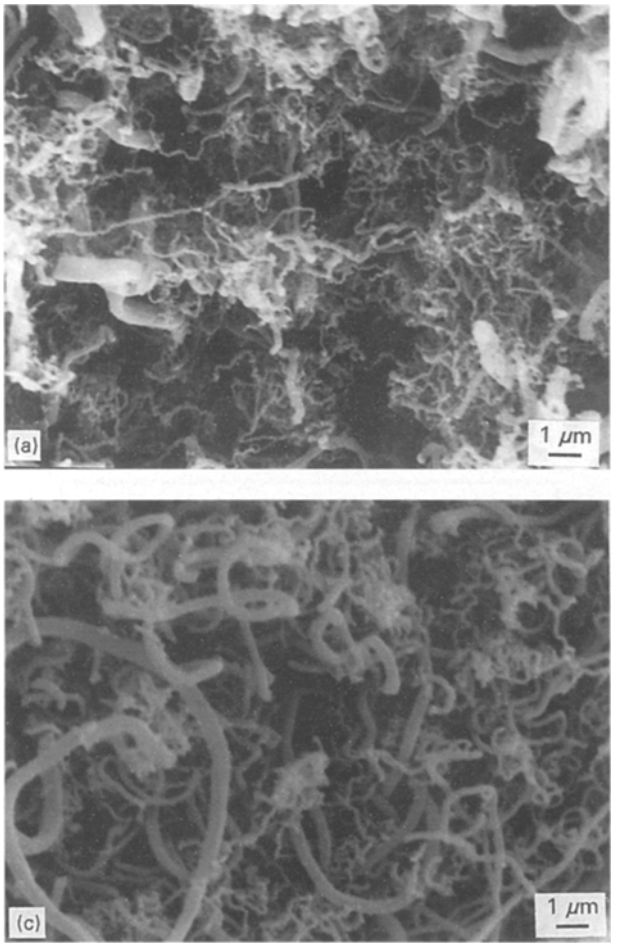

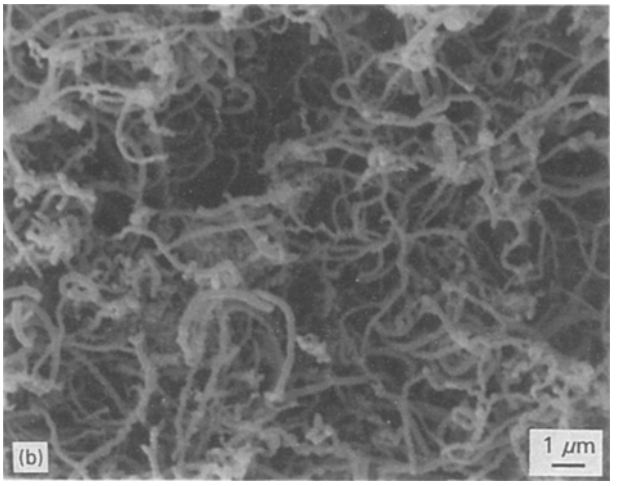

Figure 3 Electron micrographs of CCVD carbon whiskers grown at (a) 400 °C, (b) 500 °C and (c) 600 °C.

diameter of 0.5 μm. Moreover, the aspect ratio of 600 °C CCVD whiskers seems to be slightly larger than that of the 500 °C CCVD grown whiskers.

3.2. Morphology of carbon whisker–elastomer composites

The morphology of the composites is shown in Fig. 4. Electron micrographs indicate that the carbon whiskers tend to form agglomerates but the whiskers themselves are coated with the polymeric film. This was due to the processing procedure of the composites (as the TPE pellets were dissolved in chloroform and mixed with the carbon whiskers). The electron tunnelling-based conduction, explained in the later sections is based on the formation of such a polymeric film coating on the carbon whiskers. (The C–P–C junction based conduction phenomenon is based on this morphological observation.) The carbon whiskers were dispersed better in 400 °C, 52 vol % and 500 °C, 33 vol % fraction composites than those in 500 °C, 52 vol % and 600 °C, 33 vol % fraction composites. It will be shown in the following sections that the electrical and mechanical properties of the composites were controlled by their morphology.

3.3. Dynamic mechanical thermal analysis of carbon whisker–elastomer composites

The complex Young's modulus E^* and the tan δ of the elastomer were observed as a function of temperature. Similar observations were made for 500 °C, 33 vol% whisker fraction composites and are given in Fig. 5. For dynamic modulus measurements such as shown in Fig. 5, T_g can be identified as the onset of long-range co-ordinated motion of polymer molecules. A sudden drop in modulus and a maxima of tan δ around −50 °C correspond to the T_g of the EB segments of the S–EB–S copolymer. This peak compared well with the 500 °C, 33 vol % fraction composites data. Although, the addition of whiskers altered the properties such as modulus and damping coefficient of the composites it did not alter the T_g of the TPE.

3.4. Tensile deformation characteristics of carbon whisker–elastomer composites

Representative stress–strain behaviour of the composites is given in Fig. 6 and summarized in Table I. The tensile modulus depends on the deposition temperature and the concentration of the whiskers. As the deposition temperature increased, the whiskers became more needle-like and hence stronger and possibly more brittle. The 400 °C, 52 vol % and 500 °C, 33 vol % fraction whisker composites deformed homogeneously. The initial portion of the stress–strain curve was linear followed by a gradual reduction in the slope as the deformation continued, reflecting the deagglomeration and decohesion of the whisker from the elastomeric matrix. These two mechanisms were believed to be responsible for the initiation of microcracks which led to the final failure of the composites.

A low failure strain was observed with the composites containing 600 °C, 33 vol % whiskers that are characterized by a needle-like whisker morphology. Internal flaws were developed in this sample which failed at a much lower strain as compared with those of the composite containing 500 °C, 33 vol % fraction whiskers. The presence of large number of whiskers 500 °C, 52 vol % reduced the interparticle width between the whiskers and thereby prevented them from deforming homogeneously. This resulted in high modulus and low strain values.

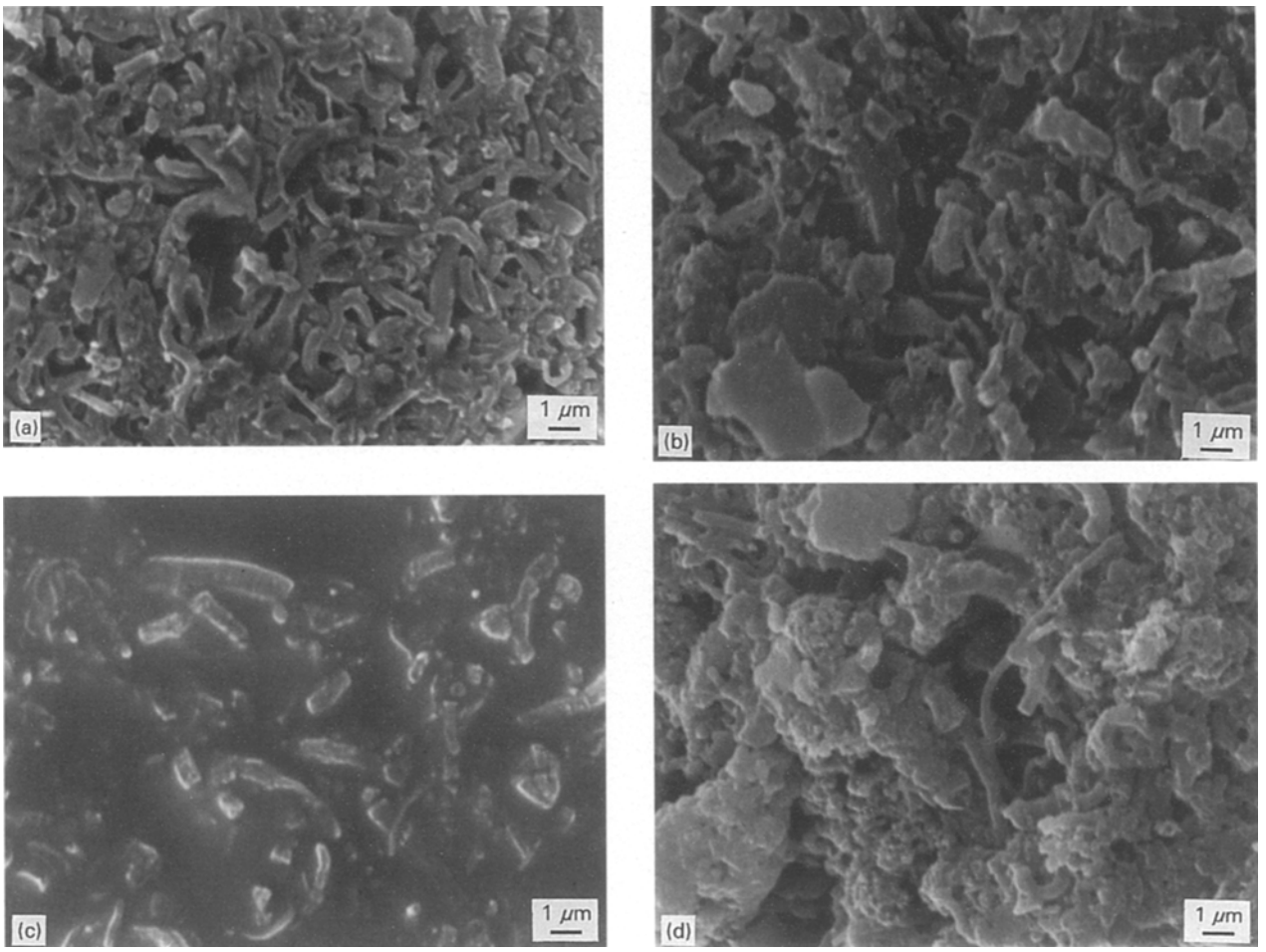

Figure 4 Morphology of carbon whiskers–elastomer composites: (a) 400 °C, 52 vol % fraction; (b) 500 °C, 33 vol % fraction; (c) 500 °C, 52 vol % fraction and (d) 600 °C, 33 vol % fraction.

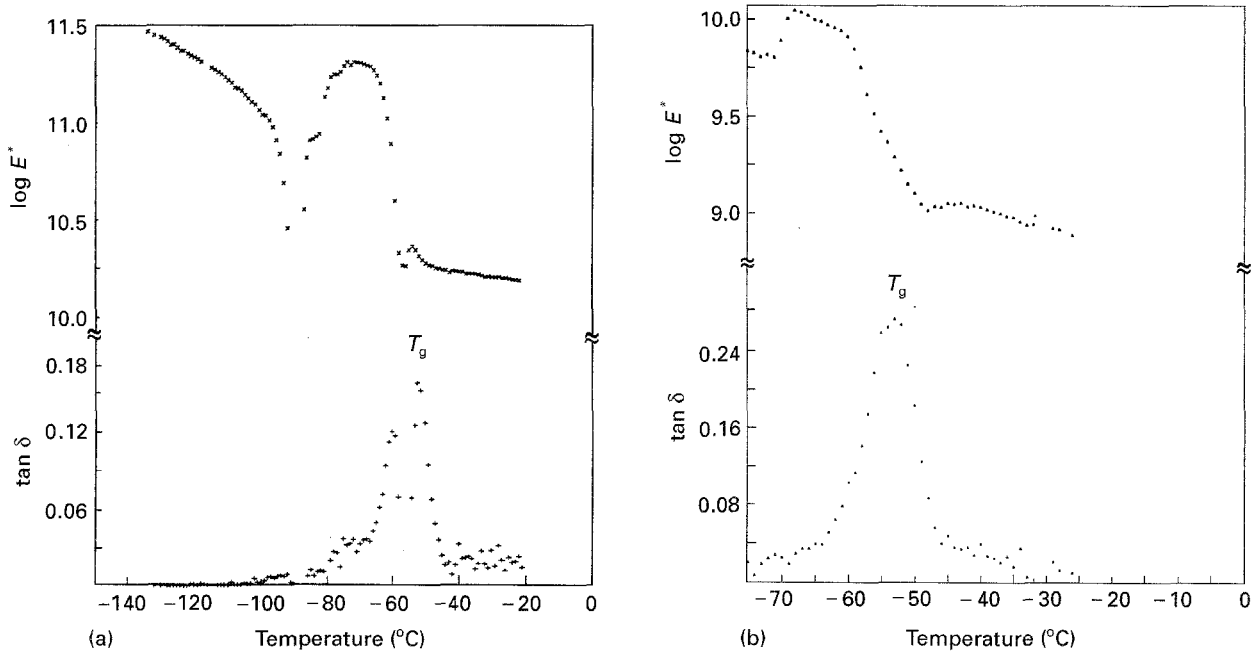

Figure 5 Dynamic mechanical thermal analysis of (a) elastomer and (b) 500 °C, 33 vol % whisker composites.

Electron micrographs of the fracture surface of the composites are shown in Fig. 7. Carbon whiskers were pulled out in 600 °C, 33 vol % and 500 °C 52 vol % fraction composites. This was due to the large entanglements (agglomeration) of the whiskers which acted as stress concentration points. In contrast 500 °C, 33 vol % and 400 °C, 52 vol % composites had uniform fracture surface with no noticeable pull-out or whisker entanglements. This was consistent with the observed large strain values. The tensile deformation behaviour is sensitive to the morphology developed as can be inferred from Figs 4, 6 and 7. The

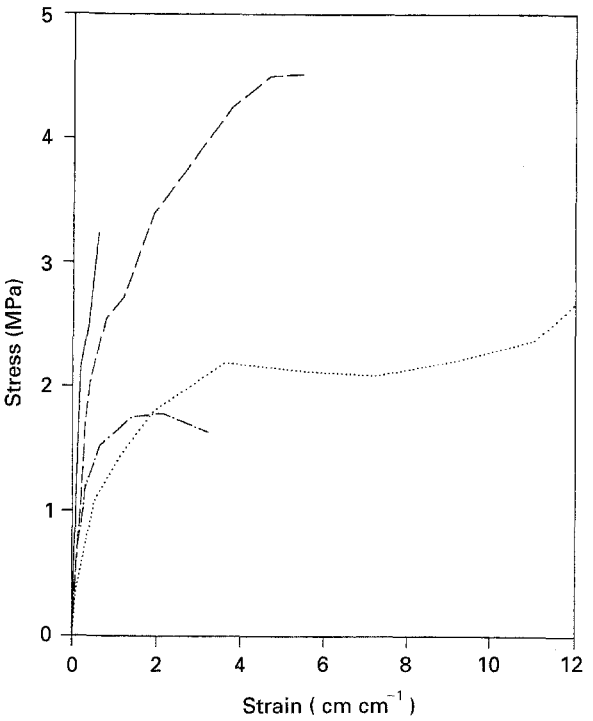

Figure 6 Stress–strain curves of carbon whisker–elastomer composites: (- - - -) 400 °C, 52 vol % fraction; (····) 500 °C, 33 vol % fraction; (——) 500 °C, 52 vol % fraction; (- · - · -) 600 °C, 33 vol % fraction.

strength and failure strain of these composites depend not only on the constituent properties but also on the adhesive strength between the whisker and the elastomer and the interparticle distance between them.

3.5. D.c. conduction characteristics of carbon whisker–elastomer composites

3.5.1. Resistivity versus strain

Representative electrical resistivity versus strain data of the samples is shown in Fig. 8. As the deformation continued, the resistivity of the composites increased exponentially and it closely followed the tensile deformation behaviour. The resistivity of composites containing 400 °C, 52 vol % fraction whiskers increased with the increasing strain (i.e. from $10^1\Omega$ cm to 10^5 cm). The resistivity increased from 10^1 to $10^3\,\Omega$ cm with an increasing strain up to the 1 cm cm^{-1} in the linear portion of the stress–strain curve. After the sample reached the non-linear portion of the stress–strain curve, the resistivity increased from 10^3 to $10^5\,\Omega$ cm as the strain increased from 1 to 4 cm cm^{-1}.

The resistivity–strain plot of 500 °C, 33 vol % fraction whisker composites showed two distinct plateau regions and can be compared to their tensile

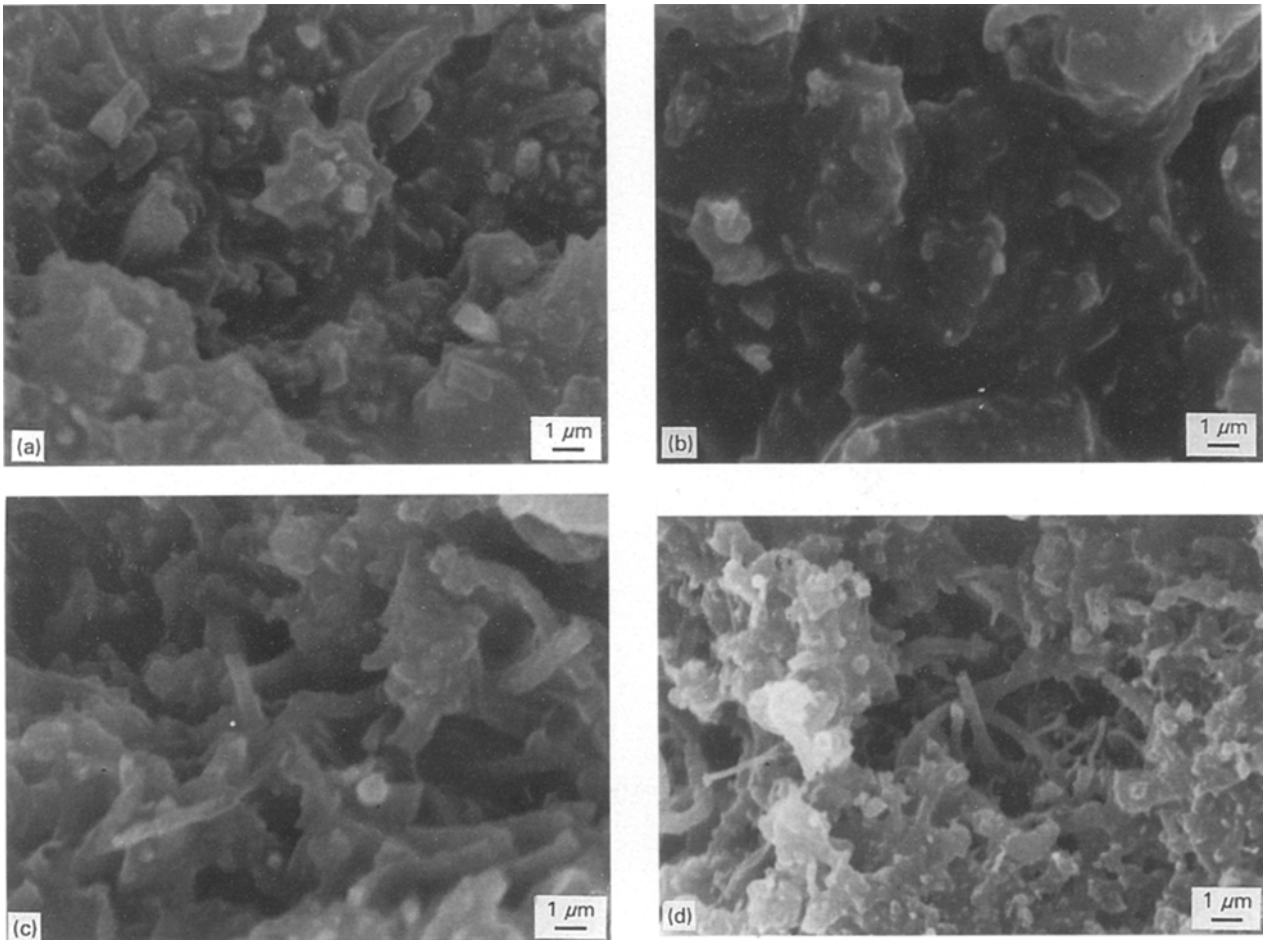

Figure 7 Electron micrographs of the fracture surface of carbon whisker–elastomer composites: (a) 400 °C, 52 vol % fraction; (b) 500 °C, 33 vol % fraction; (c) 500 °C, 52 vol % fraction; (d) 600 °C, 33 vol % fraction.

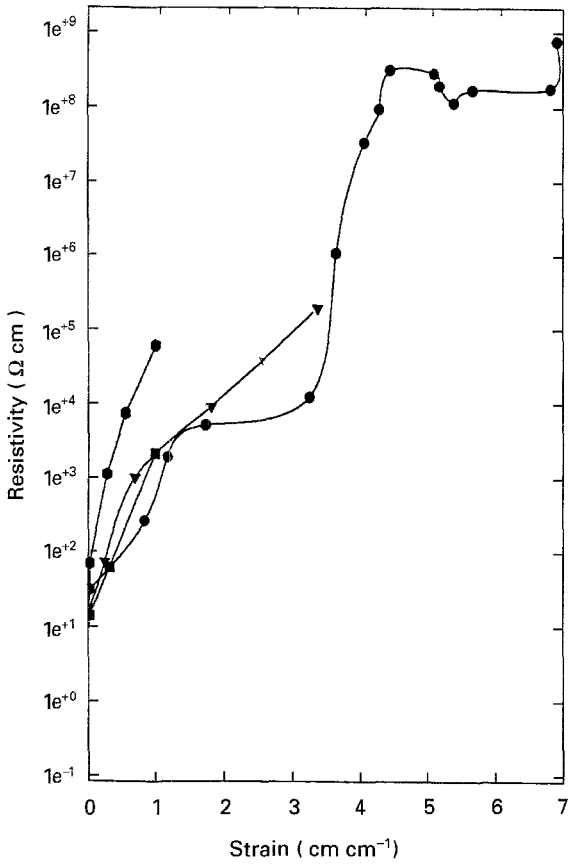

Figure 8 Resistivity as a function of strain for carbon whisker–elastomer composites: (▼) 400 °C, 52 vol % fraction; (●) 500 °C, 33 vol % fraction; (■) 500 °C, 52 vol % fraction; (⬢) 600 °C, 33 vol % fraction.

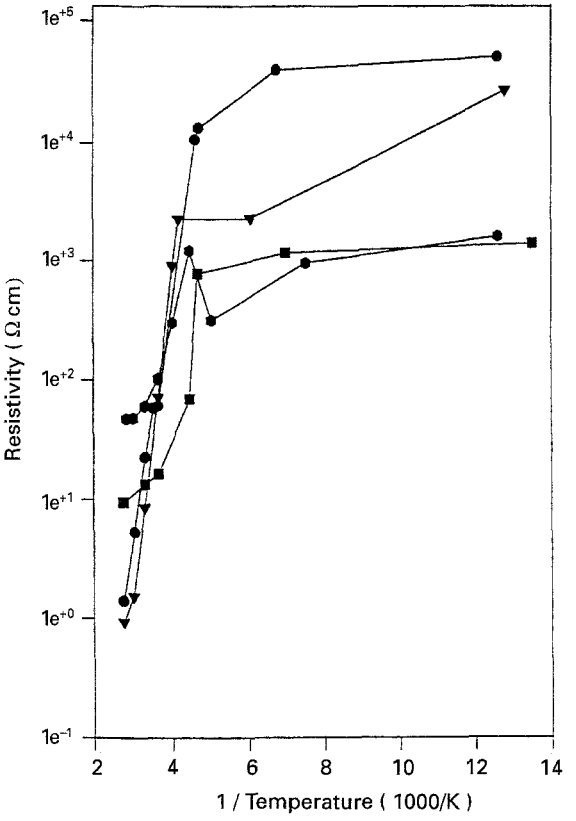

Figure 9 Resistivity as a function of temperature for carbon whisker–elastomer composites: (▼) 400 °C, 52 vol % fraction; (●) 500 °C, 33 vol % fraction; (■) 500 °C, 52 vol % fraction; (⬢) 600 °C, 33 vol % fraction.

deformation behaviours. The whisker agglomerates continuously changed with the applied strain. In the initial stage up to 1–2 cm cm^{-1} strain no debonding was observed and the resistivity changed only by two orders of magnitude (i.e. from 10^1 to $10^3\,\Omega$ cm). At about 3–4 cm cm^{-1} strain, debonding between the agglomerates and the elastomer was observed. This was accompanied by a sudden change in resistivity from 10^3 to $10^8\,\Omega$ cm. In the final deformation stage, the deagglomerated whiskers started to become oriented and the resistivity remained almost constant ($\sim 10^8\,\Omega$ cm) with increasing strain.

The resistivity of the composites featuring 600 °C, 33 vol % fraction whiskers increased exponentially (linearly, from 10^{12} to $10^5\,\Omega$ cm), mainly due, however to the internal flaws and discontinuities. Similar exponential rise in resistivity 10^1 to $10^4\,\Omega$ cm) was observed for 500 °C, 52 vol % fraction composites. The resistivity versus strain curves had similar slopes to the stress–strain curves.

3.5.2. Resistivity versus temperature

A plot of resistivity as a function of temperature (ρ versus $1/T$) is given in Fig. 9. The resistivity decreased with increasing temperature (negative temperature coefficient or NTC) with the curve exhibiting two distinct regions which were separated near the T_g($\sim$ − 50 °C) of EB segments. This observation suggests that the resistivity depends on the physical property of the TPE (see also Fig. 5). The thermal activation energy values (ΔE_A) associated with these two slopes were evaluated by using Equation 1 from Fig. 9 and are given in Table II.

TABLE II Activation energies of carbon whisker–elastomer composites

Vol fraction (%)	Temperature (°C)	Activation energy, ΔE_I (eV)	Activation energy, ΔE_{II} (eV)
33	600	0.055	0.153
33	500	0.067	0.240
52	500	0.030	0.138
52	400	0.180	0.260

Region I: $T < 230$ K, and
Region II: $T > 230$ K.

$$\ln \rho = \ln \rho_0 + (\Delta E_A / kT) \quad (1)$$

where ρ_0 = the resistivity constant which depends on the effective interparticle distance and the tunnelling nature of the TPE. The origin of ρ_o will be discussed in section 4 with respect to Equation (4).

Table II shows that the activation energy of region I ($T < T_g$) varies from 0.030 to 0.180 eV whereas the activation energy of region II ($T > T_g$) is of the order 0.138 to 0.260 eV. Moreover 600 °C, 33 vol % fraction composites exhibited switching or a positive temperature coefficient of resistivity (PTCR) near − 50 °C. This type of PTCR effect has been attributed to nonlinear conduction [20–21] and may lead at high fields to Schotkky type internal field emission [22]. The above observations indicated that the conduction

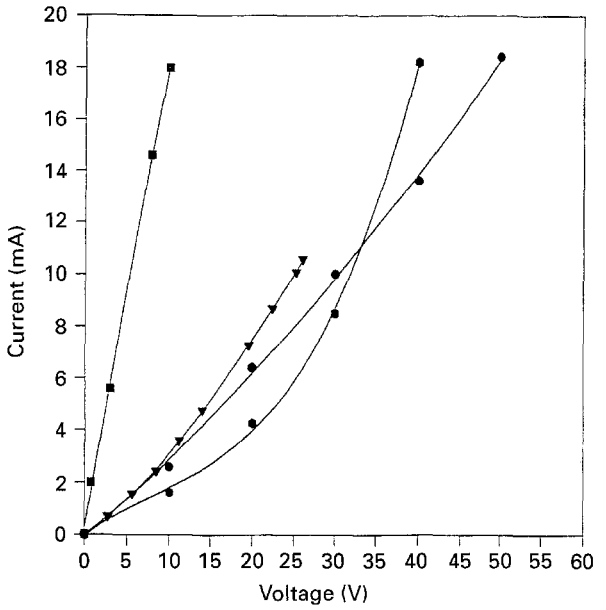

Figure 10 Voltage–current characteristics of carbon whisker–elastomer composites: (▼) 400 °C, 52 vol % fraction; (●) 500 °C, 33 vol % fraction; (■) 500 °C, 52 vol % fraction; (⬢) 600 °C, 33 vol % fraction.

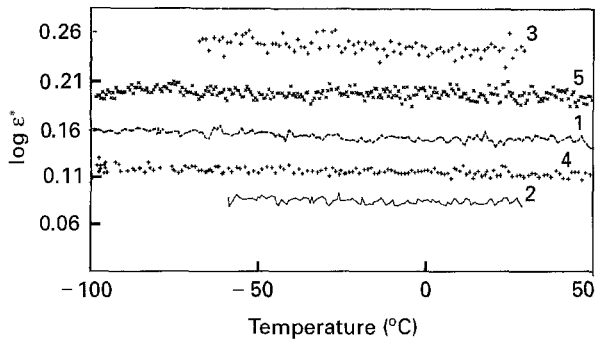

Figure 11 Dielectric constant, ε* of (1) elastomer; (2) 400 °C, 52 vol % fraction; (3) 500 °C, 33 vol % fraction; (4) 500 °C, 52 vol % fraction; (5) 600 °C, 33 vol % fraction carbon whisker–elastomer composites.

between carbon whiskers occurs through the elastomer in these composites.

3.5.3. V–I characteristics

The *V–I* characteristics of the composites are shown in Fig. 10. All the samples except 600 °C, 33 vol % whisker fraction composites exhibited some non-linearity at high voltage. This was the same sample which exhibited a PTCR effect as shown in Fig. 9. It has been reported [23] that non-ohmic behaviour is associated with localized field strength. The localized field strength arises due to the presence of local discontinuities. In narrow insulating polymer gaps between conducting areas of carbon whiskers high field strengths may develop which can lead to the observed non-ohmic behaviour such as in 600 °C, 33 vol % whisker composites.

3.6. Dielectrical thermal analysis

The dielectric constant ε*, tan Δ and loss current ε″ are plotted as a function of temperature in Figs 11 and 12, respectively. The capacitance (*C*) and the dielectric constant (ε*) of the composites are summarized in Table III. The ε* of the composites had a similar behaviour to that of the pure elastomer and

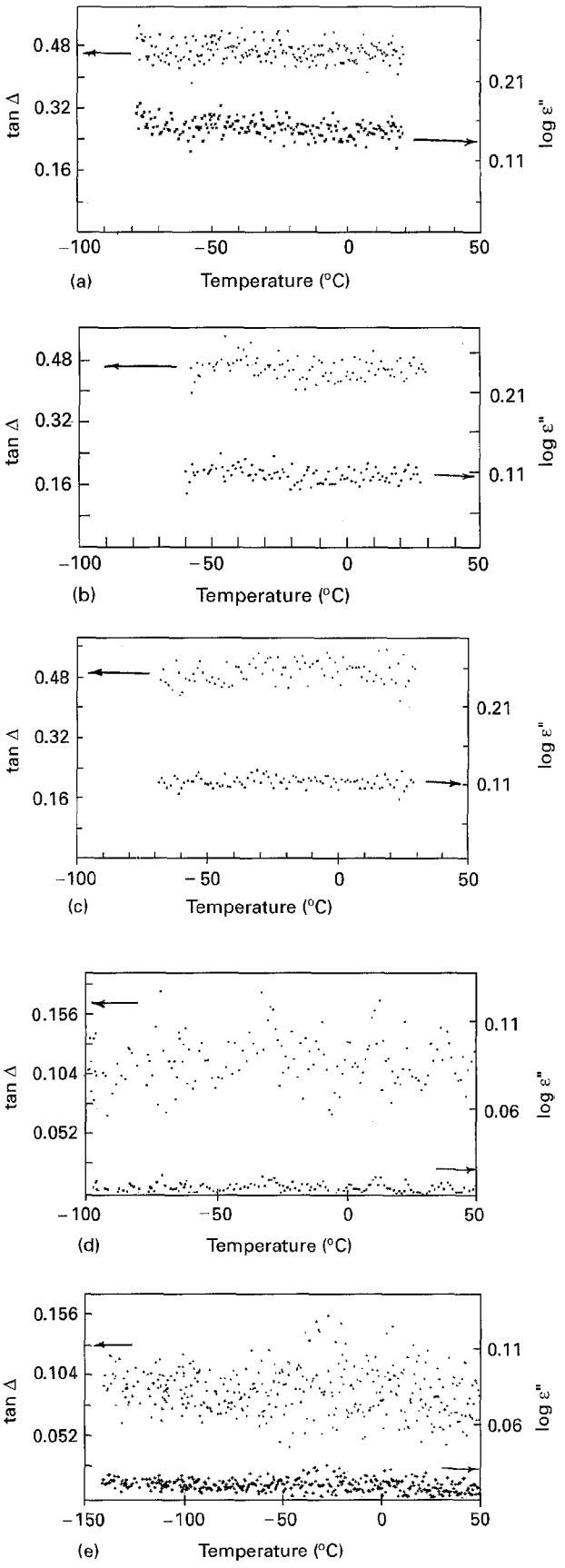

Figure 12 Dielectric loss tan Δ and ε″ of (a) elastomer; (b) 400 °C, 52 vol % fraction; (c) 500 °C, 33 vol % fraction; (d) 500 °C, 52 vol % fraction and (e) 600 °C, 33 vol % fraction carbon whisker–elastomer composites.

TABLE III Dielectric properties of carbon whisker–elastomer composites

Vol fraction (%)	Temperature (°C)	Relative permittivity (ϵ_r)	Capacitance ($pF\,mm^{-1}$)	Resistivity 20 °C (Ω cm)
33	600	1.578	47.84	69.04
33	500	1.762	27.24	31.07
52	500	1.320	111.13	13.93
52	400	1.226	232.25	18.76

was constant over the whole temperature range (Fig. 11). It is possible to have the dielectric constant independent of temperature especially in co-polymers such as our elastomer, where polystyrene is non-polar and the EB segments are polar. Though some interfacial polarization was observed in some composites due to the heterogeneities present, the samples exhibited a low tan Δ and ε'' value. When the charge carriers are trapped between the whiskers inside the polymer (such as a C–P–C junction), field distortions may occur which leads to an increased capacitance. This was observed in 400 °C, 52 vol % and 500 °C, 52 vol % composites; however, the dielectric constant remained almost the same. This is a clear indication of the effect of interfacial polarization. Also the dielectric properties of the composites reflected the dielectric behavior of the polymer indicating that conduction in these composites could occur through several C–P–C junctions.

4. Discussion

The conduction process of carbon whisker–elastomer composites was controlled by the conductivity of the whisker, nature of the polymer and the effective gap between the conducting whisker elements. This in turn was dictated by the morphology of the composites. The measured properties of the composites can be classified into two groups:

Group I. 500 °C, 33 vol % and 400 °C, 52 vol % fraction composites: high failure strain, high activation energy, high tan Δ and ε'' values (close to those of the elastomer).
Group II. 600 °C, 33 vol % and 500 °C, 52 vol % fraction composites: low failure strain, low activation energy, low tan Δ and ε'' values.

In general the electrical conduction depends on the microstructure of the composites and could take place through the following ways:

1. The carbon whiskers are separated within the agglomerates and the agglomerates themselves are separated.
2. The whiskers in the agglomerates are continuous but the agglomerates themselves are separated by the elastomer.
3. The carbon whiskers are separated within the agglomerates but the agglomerates are interconnected.

Depending on the type of whisker concentration, dispersion and the aspect ratio one would find a variety of the above combinations. This is evident from the morphology of the composites (Fig. 4). The temperature–resistivity plots (Fig. 9) exhibit two different slopes intersecting at the T_g of the TPE elastomer: Region I, $T < 230$ K and Region II, $T > 230$ K, where the activation energy of Region II is greater than that of Region I (Table II). Further, the PTCR effect of the composites with 600 °C, 33 vol % fraction whiskers near T_g of the elastomer lead us to believe that there may be a conduction barrier, like carbon–polymer–carbon junction (C–P–C) in the composite and the conduction between whiskers occurs by electron tunnelling or hopping.

When free electrons try to cross this insulating barrier they are trapped by the elastomer. The probability of electrons reaching the other side depends on the thermal fluctuations of the polymer itself. Qualitatively it can be said that while only a few chain atoms (1–5) fluctuate below the T_g, some 10–50 chain atoms attain sufficient thermal energy to move in a co-ordinated manner above the T_g. This has been observed by Miyamoto and Shibayama [24] for polystyrene, polymethyl methacrylate and an unsaturated polyester.

Based on the above observation a general model developed by Mott for hopping will be applied to the conduction behaviour of the composites [25]. The probability $P(e)$ of an electron crossing a potential barrier is given by the following relation

$$P(e) = a\tau\exp(-\Delta E_A/kT) + \exp(\Delta E_P/kT) \quad (2)$$

where ΔE_P = the normal polarization energy, ΔE_A = the activation energy for the insulating barrier, a = material constant and τ = the tunnelling factor given as

$$\tau = \exp(-Bw) \quad (3)$$

where B = the material constant for tunnelling, w = the effective interparticle width. For long samples, the polarization factor can be neglected. Therefore, the resistivity depends on the average gap width and the temperature as shown below

$$\rho \propto \exp(Bw)\, X \exp(\Delta E_A/kT) \quad (4)$$

Hence the resistivity in the bulk sample can be increased exponentially by increasing the effective gap width of the C–P–C junction or increasing the energy barrier for electron transport. The former was achieved by uniaxial stretching where the effective interparticle distance was continuously changed. The latter was achieved by varying the temperature thus modulating the energy barrier for tunnelling conduction.

5. Conclusions

1. The observed electrical conduction behaviour of highly loaded CCVD carbon whisker reinforced TPE composites was contributed by electron tunnelling, which was confirmed by the temperature–resistivity studies. The electrical property of the composites depends on the physical property of the elastomer, quality of the carbon whiskers and the morphology of the composites.

2. CCVD carbon whisker can be used to increase the mechanical and electrical properties of thermoplastic elastomers. The electrical resistivity of such composites can be increased exponentially by tensile deformation (10^1 to 10^{5-8} Ω cm) or by temperature (10^1 to 10^5 Ω cm). The deformation and temperature sensitive conduction properties can be useful in electromechanical and electrothermal device applications.

Acknowledgement

Financial support by the US-NSF Materials Engineering and Tribology Program is gratefully acknowledged.

References

1. W. F. VERHELST, K. G. WOLTHUIS, A. VOET, P. EHRBURGER and J. B. DONNET, *Rubber Chem. Technol.* **50** (1977) 735.
2. A. VOET, *Ibid.* **54** (1981) 42.
3. J. KOST, M. NARKIS and A. FOUX, *Polymer Eng. Sci.* **23** (1983) 56.
4. D. M. BIGG, *Polym. Compos.* **8** (1987) 1.
5. P.K. PRAMANIK and D. KHASTGIR, *J. Mater. Sci.* **25** (1990) 3848.
6. S. RADHAKRISHNAN, *Polym. Commun.* **26** (1985) 153.
7. R. LANDAUER, "Electrical transport and optical properties of inhomogeneous media", edited by J. C. Garland and D. B. Tanus, (American Institute of Physics, New York, 1978) p. 2.
8. M. BLASKIEWICZ, D. S. MCLACHLAN and R. E. NEWNHAM, *Polym. Eng. Sci.* **32** (6) (1992) 421.
9. P. B. JANA, S. CHAUDHURI, A. K. PAUL and S. K. DE, *Ibid.* **32** (1992) 448.
10. S. KIRKPATRICK, *Rev. Mod. Phys.* **45** (1973) 574.
11. M. S. DRESSELHAUS, G. DRESSELHAUS, K. SUGIHARA, I. L. SPAIN and H. A. GOLDBERG, "Graphite fibers and filaments" (Springer-Verlag, Germany, 1978) p. 18.
12. G. G. TIBBETTS, *J. Cryst. Growth* **66** (1984) 632.
13. T. BAIRD, J. R. FRYER and B. GRANT, *Carbon* **12** (1974) 591.
14. N. M. RODRIGUEZ, M. S. KIM, W. B. DOWNS and R. T. K. BAKER, "Carbon fibers, filaments and composites", edited by J. L. Figueiredo, C. A. Bernardo, R. T. K. Baker and K. J. Huttinger, (Kluwer Academic Publishers, The Netherlands, 1990) p. 541.
15. J. J. BROPHY, *J. Appl. Phys.* **33** (1964) 114.
16. G. M. JENKINS and K. KAWAMURA, "Polymeric carbons–carbon fibre, glass and char" (Cambridge University Press, Cambridge, 1976) p. 86.
17. G. PAN, N. MUTO, M. MIYAMA and H. YANAGIDA, *J. Mater. Sci.* **27** (1992) 3497.
18. Z. W. CHIOU, "Catalyst assisted growth of multidirectional carbon whiskers for composite application", Ph.D. Thesis, Auburn University, Auburn, AL (1993).
19. L. K. H. VAN BEEK and B. I. C. F. VANPUL, *J. Appl. Polym. Sci.* **6** (1962) 651.
20. M. NARKIS, A. RAM and Z. STEIN, *Polym. Eng. Sci.* **21** (1981) 1049.
21. S. RADHAKRISHNAN and D. R. SAINI, *J. Mater. Sci.* **26** (1991) 5950.
22. D. L. PULFREY, A. H. M. SHOUSHA and L. YOUNG, *J. Appl. Phys.* **41** (1970) 2838.
23. J. P. REBOUL and G. MOUSSALLI, *Intern. J. Polymeric Mater.* **5** (1976) 133.
24. T. MIYAMOTO and K. SHIBAYAMA, *J. Appl. Phys.* **44** (1973) 5372.
25. N. F. MOTT, *Adv. Phys. (Philos. Mag. Suppl.)* **16** (1967) 49.

Received 12 October 1994
and accepted 22 March 1995